Published in final edited form as:
J Mol Biol. 2010 December 17; 404(5): 794–802. doi:10.1016/j.jmb.2010.10.017.

The Interaction of Capping Protein with the Barbed End of the Actin Filament

Taekyung Kim[a], **John A. Cooper**[a], and **David Sept**[b]

[a]Department of Cell Biology and Physiology, Washington University School of Medicine, St. Louis, MO 63110, USA

[b]Department of Biomedical Engineering and Center for Computational Medicine and Bioinformatics, University of Michigan, Ann Arbor, MI, 48109, USA

Abstract

The interaction of capping protein with actin filaments is an essential element of actin assembly and actin-based motility in nearly all eukaryotes. The dendritic nucleation model for Arp2/3-based lamellipodial assembly features capping of barbed ends by capping protein, and the formation of filopodia is proposed to involve inhibition of capping by formins and other proteins. To understand the molecular basis for how capping protein binds the barbed end of the actin filament, we have used a combination of computational and experimental approaches, primarily involving molecular docking and site-directed mutagenesis. We arrive at a model that supports all of our biochemical data and agrees very well with a cryo-EM structure of the capped filament. Capping protein interacts with both actin protomers at the barbed end of the filament, and the amphipathic helix at the C-terminus of the beta subunit binds to the hydrophobic cleft on actin, in a manner similar to WH2 domains. These studies provide us with new molecular insight into how capping protein binds to the actin filament.

Introduction

Actin is one of the most abundant proteins in eukaryotes and it plays a critical role in diverse cellular processes, including muscle contraction, cell division, cell polarity, cell migration, vesicle trafficking and the maintenance of the cell[1]. For all of these processes, the cell must closely regulate the assembly and disassembly of actin filaments (F-actin), and a large number of actin-binding proteins are used to achieve this level of control. Capping protein (CP), known as CapZ in muscle, is a major regulator of actin dynamics. CP binds to the barbed ends of actin filaments with a low nanomolar range affinity and “caps” the filament end by preventing addition and loss of actin subunits. CP is an essential element of the dendritic nucleation model, which explains how the branched network of actin filaments is formed at the leading edge of migrating cells by the action of Arp2/3 complex. In this model, CP binding prevents prolonged polymerization of any given actin filament, leading to the formation of short filaments that are necessary to provide force to push the cell membrane forward. CP is also important for maintaining a pool of actin monomers by

Corresponding author: David Sept, Biomedical Engineering, University of Michigan, 1101 Beal Ave., Ann Arbor, MI, 48109, T: (734) 615-9587, F: (734) 647-4834, dsept@umich.edu.

preventing excessive addition of monomeric actin to barbed ends, which would quickly deplete the pool of monomeric actin. Inhibition of CP is proposed to be important for the formation of the long unbranched actin filaments in filopodia, based on the action of formins and VASP family proteins[2].

The physiological significance of CP has been studied in several *in vivo* systems[1]. In mammalian cells, CP knockdown causes a dramatic loss of lamellipodia, a necessary component of cell motility[3]. CP null mutations in *Drosophila* are lethal at an early larval stage[4] and CP mutations in budding yeast and Dictyostelium strongly affect actin assembly[5; 6]. CP is also a required component for the motility of *Listeria* and *Shigella* in reconstituted system *in vitro*[7], and CP tethers the actin thin filaments to the Z-disc of the muscle cells and thereby plays an important role in muscle development[8]. Finally, CP interacts with the Arp1 minifilament of the dynactin complex, which is necessary for the function of the microtubule motor dynein[9].

CP is an α/β heterodimer with each subunit having a size of ~30-35 kDa. Based on X-ray crystallography, the structure of CP resembles a mushroom, with a stalk and a cap[10]. Despite very low sequence similarity, the α and β subunits have almost identical secondary structures, and they bind to each other about a two-fold rotational axis of symmetry. In the crystal structure[10] and a recent NMR structure[11], the C-terminal region of the CPα subunit lies on the top surface of the CP body; however, the C-terminal region of CPβ extends away from the body. In biochemical studies, the C-terminal region of each subunit is necessary for optimal binding to the barbed end of actin filament[12].

Polyphosphoinositides and various proteins such as V1, CD2AP, CARMIL, CKIP-1, CAPZIP and WASHCAP bind to and regulate the activity of CP[13; 14]. The molecular basis of several of these interactions have been elucidated[11; 15; 16; 17; 18], however the details of how CP interacts with the barbed end of the actin filament has been a much more challenging endeavor. A cryo-electron microscopy (cryo-EM) structure of the CP/F-actin complex was recently solved, albeit at a low resolution of 32 Å[19]. This structure clearly shows that capping protein interacts with the two actin protomers at the barbed end of the filament. Although not resolved in the structure, it was suggested that the CPβ C-terminus or “CPβ tentacle” binds in the hydrophobic cleft between subdomains 1 and 3. Other interactions between CP and the barbed end are predicted based on crystal structures docked into the cryo-EM density; however, many of the molecular interactions have not been defined or biochemically tested.

In this study, we investigate the interaction of CP with the actin filament using structure-function analysis through a combination of site-directed mutagenesis and computational approaches. We arrive at a molecular model for the CP/F-actin complex that matches well with the cryo-EM model and agrees with our biochemical data. Further, this structure confirms some of the atom level interactions predicted from the EM work, excludes other amino acids from this same model, and identifies new regions of CP that are important for capping activity. Ultimately, our new model gives a more detailed understanding of actin filament regulation by CP.

Results

Interaction of the CP body with actin

We began with a series of initial RosettaDock[20] results, the cryo-EM structure of the capped filament, and our own assessment of potentially important residues based on sequence conservation and other data. All of these data implicated helix 5 of both the CPα- and β-subunits in the interaction with actin. Both of these helices are located on the top surface of

the CP structure, and we introduced pairs of point mutations along the length of each helix and performed seeded actin polymerization assays with kinetic modeling to determine the binding affinity of these CP mutants for F-actin (Figure 1). Many of the mutations, namely CPα S234A/E238A, E223A/N227A, E241A/N245A, T241A/E245A, T249A/T253A, Q248A, D252A and CPβ R215A/D219A, N222A/S226A, T227A, N229A, K237A/D241A, E230A/G234A, K235A, and D238A only produced a 1-2 fold increase in the K_d as compared with wt CP (see Table 1). However, CPβ K223A and R225A caused more than a 3-fold increase in the K_d, indicating that these residues are likely more important for binding to actin.

We next tested whether the α-tentacle is involved in the interaction with actin. As determined previously[12], we found that CPα(ΔC28)β, a truncation of R259 to A286 in CPα, produced a 18,000-fold increase in the K_d. We also determined that a shorter truncation CPα(ΔC13)β, consisting of residues I274 to A286 in the α-tentacle, caused only a 4-fold increase in the K_d. The cryo-EM model predicted that the highly conserved basic residues in the CPα tentacle interact with CP through electrostatic binding[19]. To test this potential interaction, we introduced point mutations in the CPα tentacle. Mutations D270A and K273A produced only a 1-2 fold increase in the K_d for binding whereas mutations of highly conserved basic residues, K256A, R260A and K268A, produced more than a 6-fold increase in the K_d, consistent with the previous results[18]. R266A was also in this cluster of basic residues, but this mutation only produced a 1.5-fold increase in the K_d.

Based on these experimental findings, we re-examined our initial docking results and performed perturbation RosettaDock[20] runs to refine our model. We also looked at the single mutations that caused more than a 3-fold increase in the K_d and determined their solvent accessibility in the crystal structure and in our molecular dynamics (MD) simulation[21]. Four of the mutation sites on the CP body, CPα K256, R260, K268 and CPβ K223, were found to always be solvent exposed, but CPβ R225 was not in direct contact with solvent and appeared to be more important for maintaining the integrity of the CP dimer. Based on this, we re-ranked all of our docking results, scoring each structure based on the fraction of buried surface area for these four solvent exposed residues. This re-ranking procedure resulted in a slightly refined model for the capped barbed end and predicted new salt bridge interactions for CPα E200 and CPβ R195. The subsequent mutation of these residues (CPα E200R and CPβ R195A) resulted in K_d increases of 31.5- and 3.5-fold respectively, strongly supporting our CP/F-actin model shown in Figure 2.

Our best docking model predicted several key interaction points between CP and the last two protomers at the barbed end of the actin filament, but to optimize the sidechains of the two docking partners we performed a molecular dynamics (MD) simulation of the capped filament. From the simulation, we see that CPα K256 and R260 in the CPα tentacle form salt bridges with D292 and E167 respectively on the penultimate actin protomer (actin B-1 in Figures 3 and 4A). These residues are in the basic cluster on CP, and this interaction is consistent with what was predicted by the cryo-EM model[19]. CPα K268 does not make a salt bridge with actin, but it does form hydrogen bonds with the carbonyl oxygen of S265 on actin B-1. We also see ionic bonds between CPα E200 and K284 on the last barbed end protomer, actin B (Figure 4B), as well as CPβ R195 and K223 with E276, also on actin B (Figure 4C). Interestingly, although CPβ R225 formed interactions within the CP dimer in the crystal structure, this residue quickly flips out in the MD simulation and makes a persistent salt bridge with D288 in actin B-1 (Figure 4C). Many other amino acids obviously make up the actin binding interface, and, in all, about 5000 $Å^2$ of surface area is buried between the two subunits of CP and the two protomers of the barbed end of the filament, including contributions from the CPβ tentacle which we discuss next.

Interaction of the CPβ tentacle

In previous biochemical studies, truncation of the CPβ tentacle caused a 300-fold increase of K_d, indicating that the CPβ tentacle is critical for binding to actin[12]. Additionally, the x-ray crystal structure of CP shows that the CPβ tentacle is an amphipathic α-helix and the structure of the hydrophobic side is well conserved among the CPβ isoforms, which bind equally well to actin[10]. Based on this, it was proposed that the hydrophobic residues of this amphipathic helix, such as L262 and L266, may contribute to binding to actin[22]. We mutated the hydrophobic surface of the CPβ tentacle, and as predicted L258S, L262S and L262S each produced more than a 10-fold increase in the K_d. The hydrophilic side of this amphipathic helix is not conserved through evolution and also has an isoform-specific pattern of charge distribution[10]. We mutated pairs of these residues, E256A/N260A and E256S/N260S, and these mutations caused an increase in the K_d of only 2-3 fold, indicating that this hydrophilic region is not important for actin binding.

Docking of the isolated CPβ tentacle to the barbed end of the actin filament indicated that this amphipathic helix bound in the hydrophobic cleft between subdomains 1 and 3 of actin (Figure 5). We saw binding to both actin protomers B and B-1, but given the binding orientation for the body of CP on the barbed end (Figure 2), the last protomer (actin B) was the only viable interaction site where we could reconnect the CPβ tentacle to the rest of CP. This hydrophobic cleft in actin is a well-studied interaction site for WH2 domains[23], and the similarity between the CPβ tentacle and the WH2 containing protein ciboulot has been noted previously[19]. Indeed if we take the co-crystal structure of actin with the WH2 domain of WASp[24] and overlay the actin of that structure with our protomer B, we see that the orientation for CPβ tentacle is very similar to WASp, and many of the interacting amino acids on actin match between the two structures. The hydrophobic residues on CPβ tentacle, L258, L262 and L266, interact with I345, L346, and L349 on actin B, and many of the other residues that make up the WH2 binding site, Y143, T148, E167, G168, and T351, also appear to interact with the CPβ tentacle (Figure 5).

Discussion

In this work we have developed a molecular model for the interaction of CP with the barbed end of the actin filament through a combination of structure/function analysis of a large series of point mutations and extensive computational docking studies. The resulting model is entirely consistent with a previous cryo-EM structure[19], and it provides us with a molecular understanding of the filament capping mechanism. More than 5000 $Å^2$ of surface area is buried upon capping the filament, and if we measure the residues within 3 Å of the interface, we see that the interaction involves 49 residues from CP (18 on CPα and 31 on CPβ) and 52 residues from the actin filament (35 from actin B and 17 from actin B-1). Although a large number of amino acids make up this interface, in general the binding free energy is not evenly distributed among all contact residues[25]. We find the same situation here. Our the 45 amino acids that we mutated, only 10 showed more than a 3-fold increase in the K_d, and all of these residues make contact with the barbed end actin protomers in our model.

The 23 Å cryo-EM structure of the capped filament was a major achievement by Narita et al. [19]. If we compare our molecular model to their EM density map, we see excellent correspondence between the two (supplemental data Figure S1). Although the structures agree well at this coarse level of detail, differences become more apparent when we compare the atomic models. The cryo-EM structure predicts a much more extensive interface involving 63 residues on CP. Given this long list, it is not surprising that 9 of the 10 amino acids we identified as significant are common between the two structures – only CPα K256 was not predicted to be at the interface in the cryo-EM structure. More notably, 12 residues

that the cryo-EM models predicts to contact the barbed end (CPα K273, I274, S276-K281 and CPβ E230, K235, D238 and N241) are not at the interface in our model, and mutation of these amino acids or even the deletion of the last 13 residues of the CPα tentacle resulted in a minimal change to the binding affinity (see Table 1). Conversely, the binding and orientation of the CPβ tentacle is very similar between the two models, and it is very compelling that what was predicted based on sequence homology[19] matches very well with our molecular docking results. Comparisons on the actin side are much more difficult since we are not able to perform the same mutagenesis. Narita et al. reported that the hydrophobic plug of actin B clashed with the CPα tentacle in their model[19], however this is not the case in our model. Since we used F-actin models taken from an all-atom MD simulation, the hydrophobic plug assumed a wide range of conformations, and our best model has the plug interacting favorably with helix 5 of CPβ.

Other studies have also used CP mutagenesis as a means of testing the interaction of CP with the actin filament as well as other regulatory proteins. Together with their cryo-EM work, Narita et al. examined several single, double and triple mutations at four sites on CPα: E200, K256, R260 and R266[19]. They tested both alanine as well as charge reversal substitutions (E to R or K/R to E) and found generally that charge reversal was more severe than simple alanine substitution, and that double and triple mutations were increasingly more severe than single mutations. All of these results compare well with our own findings. Zwolak et al. found that several mutations in CPβ (K142E/K143E and K181E) increased the K_d for the barbed end by about 20 fold[11]. All of the residues are away from the actin binding interface in our model, and we found that alanine substitutions at positions 142 and 143 caused only minor perturbations in actin affinity while K181A appeared to affect the stability of the CP heterodimer. In previous work from our own lab, we showed that point mutations in chicken CP[12] (CPα R259A and W271R) or the equivalent sites in yeast CP[26] (CPα R239A and W251A) produced 30 to 190-fold increases in the K_d. Both of these residues appear to be important for maintaining the CP structure. CPα R259 makes a bidentate salt bridge with CPβ E221 while CPα W271 makes hydrophobic interactions with the CP body and keeps the CPα tentacle in place.

We previously showed how the sequence conservation for CPβ was higher than that for CPα[1]. If we look in more detail, we see that the conservation for the body of CPβ is higher than that for CPα; however, the sequence conservation for the tentacles is exactly the opposite (see alignments in Figure S2). Although the sequence for the CPβ tentacle is low, the pattern of hydrophobic residues at the position corresponding to L258, L262 and L266 is maintained across a wide range of species. Apart from CP, this pattern of hydrophobic residues is also conserved in WH2 containing proteins such as WAVE, WASp and WIP[23], strongly supporting the interaction we find with the hydrophobic cleft in actin. For the CPα tentacle, the interactions made by residues K256, R260 and K268 suggest a much more specific interaction, and indeed these residues are conserved across vertebrates, fungi, flies, worms and plants. The residues after CPα W271 are only weakly conserved and are not in contact with actin in our model. Correspondingly, our deletion of the last 13 amino acids of CPα only increased the K_d by a factor of 4.2.

Apart from its role in regulating actin, CP is also a component of the dynactin complex where it caps the end of the actin-like Arp1 filament[9]. Arp1 has about 54% identity with actin and readily binds conventional actin[9], and there is evidence that the barbed end of the Arp1 filament may contain one actin protomer[27; 28]. If we look at the contact points on actin for the residues we identified as significant on the body of CP, we see that the interaction sites on actin B-1, the second to last monomer, are largely conserved in Arp1 with the exception of D292 which becomes a threonine in Arp1. The glutamate at position 167 is conserved between muscle actin and Arp1, but it corresponds to an alanine in yeast actin.

This would eliminate the salt bridge we observe in our model and may contribute to the lower affinity of yeast CP for yeast actin as opposed to muscle actin[26]. For the last protomer, actin B, there are two potentially important sequence changes – A/E at position 272 and N/F at 280 for the actin and Arp1 sequences respectively (see Figure S3). These sequence differences could alter the binding affinity of CP to a purely Arp1 filament, however since the CPβ tentacle provides a significant fraction of the overall interaction energy and the hydrophobic cleft of actin appears to be conserved in Arp1, this difference may not be very selective for Arp1 versus actin as the last protomer in the filament.

In conclusion, we have developed a molecular model for CP on the barbed end of the actin filament. Through a combination of extensive mutagenesis and docking studies, we arrived at a model that agrees extremely well with previous cryo-EM work and supports a wide range of biochemical studies. These mutagenesis results and the molecular model will both prove useful in future studies aimed at the regulation of CP by proteins such as V1/myotrophin and CARMIL.

Materials and Methods

Plasmid construction, Mutagenesis and Protein Purification

A His-tagged mouse CP alpha1/beta2 expression construct was kindly provided by Drs. Ville Paavilainen and Pekka Lappalainen (University of Helsinki, Finland). CP mutations were generated in this plasmid by site-directed mutagenesis using the Quickchange method (Stratagene, La Jolla, CA). The resulting plasmids were verified by DNA sequencing of the region of interest. For four plasmids, the entire coding region was sequenced, and no errors were found. CP, actin, and spectrin-actin seeds were purified as described previously[13].

Actin Polymerization Assays

Pyrene-actin polymerization assays, including capping by CP, were performed as described[12; 29]. For a total volume of 200 μL, actin subunits (5% pyrene labeled) at 1.5 μM in G-buffer were primed with Mg^{2+}. Then, 10 μL of 20X KME buffer (200 mM Tris / HCl pH7.5, 1M KCl, 20 mM $MgCl_2$, 20 mM EGTA) and 20 μl of spectrin-actin seeds were added[13]. For capping assays, CP was added to the mixture at time zero and the concentration of CP was varied. Binding constants for CP were determined by least-squares fitting of the data using Berkeley Madonna 8.3 (www.berkeleymadonna.com), based on the following mechanism.

$$\text{Reaction 1} \quad A + N_b \underset{k_-}{\overset{k_+}{\rightleftharpoons}} A \cdot N_b$$

$$\text{Reaction 2} \quad N_b + CP \underset{k_{-cap}}{\overset{k_{+cap}}{\rightleftharpoons}} CP \cdot N_b$$

In these reactions, A is actin monomer, N_b is a free barbed end, CP is capping protein, and $CP{\cdot}N_b$ is a capped barbed end. These equations assume that a capped barbed end, $CP{\cdot}N_b$, can neither add nor lose actin subunits. For the elongation rate constants in Reaction 1, k_+ was 11.6 $\mu M^{-1}s^{-1}$ and k_- was 1.4 s^{-1} [30]. The rate constants for capping in Reaction 2 were determined by fitting the experimental data for seeded actin polymerization with a series of concentrations of CP.

Molecular Dynamics and Docking Studies

In preparation for docking studies, we first performed separate molecular dynamics (MD) simulations on CP and the actin filament. The CP simulation was 20 ns in length and was previously described[21; 31]. For the actin filament, we constructed an 8-protomer filament based on the Oda F-actin model[32]. Using NAMD[33], we performed a 100 ns simulation using the CHARMM27 force field, an NpT ensemble at 1 atm pressure, a temperature of 300 K, a 10 Å cutoff for van der Waals interactions with a switching distance of 8.5 Å and Particle Mesh Ewald for long-range electrostatics. We extracted 5 CP and 10 F-actin structures from the MD simulations and used each combination of CP/F-actin in RosettaDock studies[20]. Since the CPβ tentacle was highly mobile in the MD simulation, we separated it from the CP body and docked the two pieces independently, ignoring the flexible linker between the two (residues S245 to D251). Further, to save on computation we only used the 3 protomers from the barbed end of the filament in our docking studies with both the CPβ tentacle and the CP body. We started each run with the CP body separated from the barbed end of the trimer by about 15 Å, and the actin trimer and CP body were randomly rotated about the line connecting their centers of mass. Our initial docking runs for the CP body involved 100 runs of each possible complex, resulting in a total of 5000 predictions. These structures were analyzed in terms of our mutagenesis results, looking for salt bridges between CP and the barbed end or just burying of the residues at the interface. We selected the best structure and performed 10,000 perturbation runs using the default dock_pert parameters in RosettaDock: up to 3 Å random perturbation along the line connecting the centers of mass, up to 8 Å random perturbation in the plane perpendicular to this line, and up to 8° random rotation around this same line connecting the centers. All of the perturbation results were then re-ranked based on the fraction of buried surface area and hydrogen or ionic bonds for the significant residues highlighted in Table 1. The best structure resulting from this analysis predicted new interactions sites that were verified by mutagenesis. For the CPβ tentacle we followed the same initial docking protocol, however the clustering of the docking results was completely unambiguous, and we were able easily identify the interaction site as the hydrophobic cleft on actin. Taking the docked positions of the CP body and CPβ tentacle, we rebuilt the flexible linker between the two using Rosetta[34]. We performed MD simulation of the final capped filament again using NAMD. The parameters were identical to those described above and after equilibration, the production run was a total of 10 ns. All molecular images were produced using VMD[35].

Supplementary Material

Refer to Web version on PubMed Central for supplementary material.

Acknowledgments

We thank Drs. Ville Paavilainen and Pekka Lappalainen for providing the His-tagged mouse CP alpha1/beta2 expression construct, Dr. Akihiro Narita for providing the cryo-EM maps for the capped filament, and Shatadal Ghosh for help with simulations. This work was supported by grants from the National Institutes of Health GM38542 (to JAC) and GM67246 (to DS).

References

1. Cooper J, Sept D. New insights into mechanism and regulation of actin capping protein. Int Rev Cell Mol Biol. 2008; 267:183–206. [PubMed: 18544499]
2. Chesarone MA, DuPage AG, Goode BL. Unleashing formins to remodel the actin and microtubule cytoskeletons. Nat Rev Mol Cell Biol. 2009; 11:62–74. [PubMed: 19997130]
3. Mejillano MR, Kojima S, Applewhite DA, Gertler FB, Svitkina TM, Borisy GG. Lamellipodial versus filopodial mode of the actin nanomachinery; pivotal role of the filament barbed end. Cell. 2004; 118:363–73. [PubMed: 15294161]

4. Hopmann R, Cooper J, Miller K. Actin organization, bristle morphology, and viability are affected by actin capping protein mutations in Drosophila. J Cell Biol. 1996; 133:1293–305. [PubMed: 8682865]
5. Amatruda J, Cannon J, Tatchell K, Hug C, Cooper J. Disruption of the actin cytoskeleton in yeast capping protein mutants. Nature. 1990; 344:352–4. [PubMed: 2179733]
6. Hug C, Jay PY, Reddy I, McNally JG, Bridgman PC, Elson EL, Cooper JA. Capping protein levels influence actin assembly and cell motility in *Dictyostelium*. Cell. 1995; 81:591–600. [PubMed: 7758113]
7. Loisel TP, Boujemaa R, Pantaloni D, Carlier MF. Reconstitution of actin-based motility of Listeria and Shigella using pure proteins. Nature. 1999; 401:613–616. [PubMed: 10524632]
8. Schafer DA, Hug C, Cooper JA. Inhibition of CapZ during myofibrillogenesis alters assembly of actin filaments. Journal of Cell Biology. 1995; 128:61–70. [PubMed: 7822423]
9. Schroer TA. Dynactin. Annu Rev Cell Dev Biol. 2004; 20:759–79. [PubMed: 15473859]
10. Yamashita A, Maeda K, Maeda Y. Crystal structure of CapZ: structural basis for actin filament barbed end capping. EMBO J. 2003; 22:1529–38. [PubMed: 12660160]
11. Zwolak A, Fujiwara I, Hammer JA, Tjandra N. Structural basis for capping protein sequestration by myotrophin (V-1). J Biol Chem. 2010
12. Wear M, Yamashita A, Kim K, Maeda Y, Cooper J. How capping protein binds the barbed end of the actin filament. Curr Biol. 2003; 13:1531–7. [PubMed: 12956956]
13. Hernandez-Valladares M, Kim T, Kannan B, Tung A, Aguda A, Larsson M, Cooper J, Robinson R. Structural characterization of a capping protein interaction motif defines a family of actin filament regulators. Nat Struct Mol Biol. 2010; 17:497–503. [PubMed: 20357771]
14. Fujiwara I, Remmert K, Hammer J. r. Direct observation of the uncapping of capping protein-capped actin filaments by CARMIL homology domain 3. J Biol Chem. 2010; 285:2707–20. [PubMed: 19926785]
15. Takeda S, Minakata S, Koike R, Kawahata I, Narita A, Kitazawa M, Ota M, Yamakuni T, Maeda Y, Nitanai Y. Two distinct mechanisms for actin capping protein regulation--steric and allosteric inhibition. PLoS Biol. 2010; 8:e1000416. [PubMed: 20625546]
16. Zwolak A, Uruno T, Piszczek G, Hammer JA 3rd, Tjandra N. Molecular basis for barbed end uncapping by the carmil homology (CAH) domain 3 of mouse carmil-1. J Biol Chem. 2010
17. Hernandez-Valladares M, Kim T, Kannan B, Tung A, Aguda AH, Larsson M, Cooper JA, Robinson RC. Structural characterization of a capping protein interaction motif defines a family of actin filament regulators. Nat Struct Mol Biol. 17:497–503. [PubMed: 20357771]
18. Kim K, McCully M, Bhattacharya N, Butler B, Sept D, Cooper J. Structure/Function Analysis of the Interaction of Phosphatidylinositol 4,5-Bisphosphate with Actin-capping Protein: Implications for How Capping Protein Binds the Actin Filament. J Biol Chem. 2007; 282:5871–9. [PubMed: 17182619]
19. Narita A, Takeda S, Yamashita A, Maeda Y. Structural basis of actin filament capping at the barbed-end: a cryo-electron microscopy study. EMBO J. 2006; 25:5626–5633. [PubMed: 17110933]
20. Gray JJ, Moughon S, Wang C, Schueler-Furman O, Kuhlman B, Rohl CA, Baker D. Protein-protein docking with simultaneous optimization of rigid-body displacement and side-chain conformations. J Mol Biol. 2003; 331:281–99. [PubMed: 12875852]
21. Bhattacharya N, Ghosh S, Sept D, Cooper JA. Binding of myotrophin/V-1 to actin-capping protein: implications for how capping protein binds to the filament barbed end. J Biol Chem. 2006; 281:31021–30. [PubMed: 16895918]
22. Barron-Casella EA, Torres MA, Scherer SW, Heng HH, Tsui LC, Casella JF. Sequence analysis and chromosomal localization of human Cap Z. Conserved residues within the actin-binding domain may link Cap Z to gelsolin/severin and profilin protein families. J Biol Chem. 1995; 270:21472–9. [PubMed: 7665558]
23. Dominguez R. Actin-binding proteins--a unifying hypothesis. Trends Biochem Sci. 2004; 29:572–8. [PubMed: 15501675]

24. Chereau D, Kerff F, Graceffa P, Grabarek Z, Langsetmo K, Dominguez R. Actin-bound structures of Wiskott-Aldrich syndrome protein (WASP)-homology domain 2 and the implications for filament assembly. Proc Natl Acad Sci U S A. 2005; 102:16644–9. [PubMed: 16275905]
25. Bogan AA, Thorn KS. Anatomy of hot spots in protein interfaces. J Mol Biol. 1998; 280:1–9. [PubMed: 9653027]
26. Kim K, Yamashita A, Wear MA, Maeda Y, Cooper JA. Capping protein binding to actin in yeast: biochemical mechanism and physiological relevance. J Cell Biol. 2004; 164:567–80. [PubMed: 14769858]
27. Bingham JB, Schroer TA. Self-regulated polymerization of the actin-related protein Arp1. Curr Biol. 1999; 9:223–6. [PubMed: 10074429]
28. Schafer DA, Gill SR, Cooper JA, Heuser JE, Schroer TA. Ultrastructural analysis of the dynactin complex: an actin-related protein is a component of a filament that resembles F-actin. J Cell Biol. 1994; 126:403–12. [PubMed: 7518465]
29. Yang C, Pring M, Wear M, Huang M, Cooper J, Svitkina T, Zigmond S. Mammalian CARMIL inhibits actin filament capping by capping protein. Dev Cell. 2005; 9:209–21. [PubMed: 16054028]
30. Pollard TD. Rate constants for the reactions of ATP- and ADP-actin with the ends of actin filaments. J Cell Biol. 1986; 103:2747–2754. [PubMed: 3793756]
31. Goley ED, Rammohan A, Znameroski EA, Firat-Karalar EN, Sept D, Welch MD. An actin-filament-binding interface on the Arp2/3 complex is critical for nucleation and branch stability. Proc Natl Acad Sci U S A. 2010; 107:8159–64. [PubMed: 20404198]
32. Oda T, Iwasa M, Aihara T, Maeda Y, Narita A. The nature of the globular- to fibrous-actin transition. Nature. 2009; 457:441–5. [PubMed: 19158791]
33. Kale L, Skeel R, Bhandarkar M, Brunner R, Gursoy A, Krawetz N, Phillips J, Shinozaki A, Varadarajan K, Schulten K. NAMD2: Greater scalability for parallel molecular dynamics. Journal of Computational Physics. 1999; 151:283–312.
34. Rohl CA, Strauss CE, Misura KM, Baker D. Protein structure prediction using Rosetta. Methods Enzymol. 2004; 383:66–93. [PubMed: 15063647]
35. Humphrey W, Dalke A, Schulten K. VMD: Visual molecular dynamics. Journal of Molecular Graphics. 1996; 14:33–38. [PubMed: 8744570]

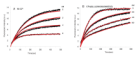

Figure 1.
Actin polymerization assays with CP mutants. Panels A and B show pyrene-actin subunits (1.5 μM, 5% pyrene label) polymerizing over time, adding to barbed ends of filaments nucleated by spectrin-actin seeds. Concentrations of CP are indicated. A: wild type CP, B: CPαβ(L258S/L262S/L266S). Experimental data are black, and fitted curves are red, based on fitting all the data to polymerization rate equations (see Methods).

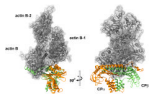

Figure 2.
Capping protein at the barbed end of the actin filament. Two views, rotated 90 degrees. The three protomers at the barbed end are shown in gray and the CP heterodimer is shown in orange (CPα) and green (CPβ).

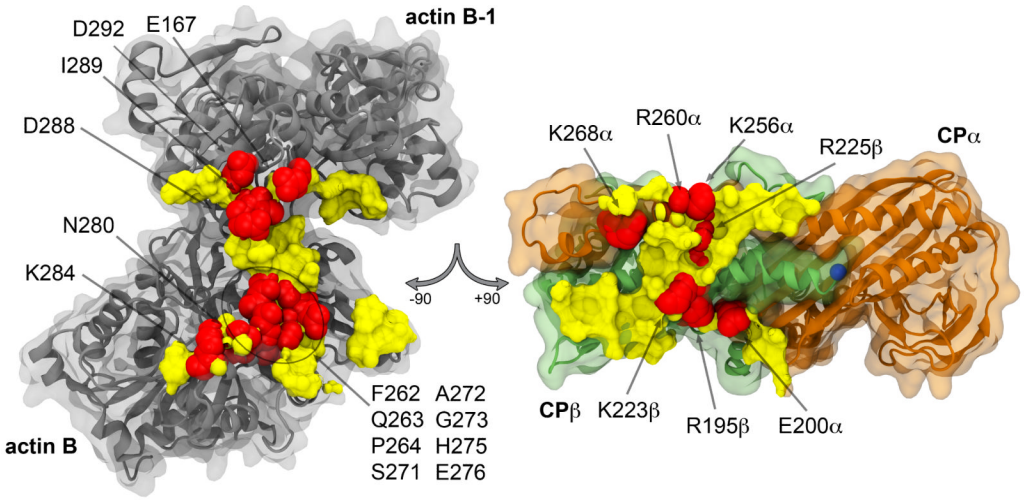

Figure 3.

The molecular details for the interaction of capping protein with the barbed end. The interacting surfaces within 3.5 Å on both the filament and CP are shown in yellow. The seven amino acids on the body of CP that were shown to have more than a 3-fold effect on the binding affinity are rendered with red van der Waals spheres. The corresponding contact residues on actin, although not tested by mutation, are also labeled and rendered as spheres. The blue sphere marks where the flexible linker to the β-tentacle was cut for docking purposes.

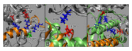

Figure 4.
Details of the ionic and hydrogen bonding interactions between CP and the barbed end of the filament. There are seven amino acids on the body of CP that contribute, including (A) CPα K256, R260 and K268, (B) CPα E200, and (C) CPβ R195, K223 and R225. Hydrogen bonds are depicted as yellow lines.

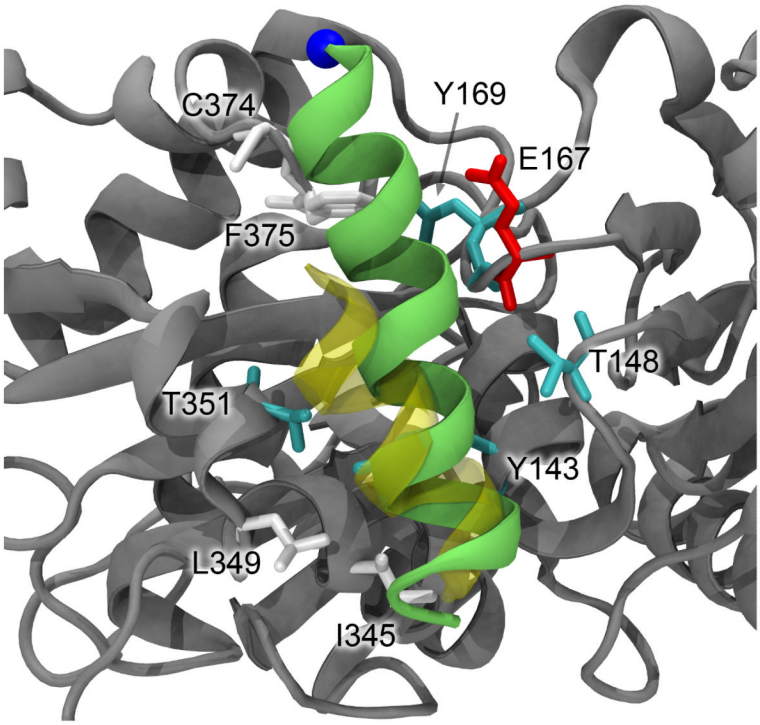

Figure 5.
The interaction of the CPβ tentacle with the hydrophobic cleft in actin. The interacting residues on actin are colored as green (polar) and white (hydrophobic). The corresponding position of the WH2 domain from WASp (pdb 2A3Z) is shown in yellow. The blue sphere marks the N-terminus of the β-tentacle where the flexible linker connected to the main body of CP.

Table 1

Summary of the mutational analysis

CP Alpha Subunits	Kd(nM)	Relative affinity (X-fold)	Location of the mutation	Conservation of the amino acid residues
WT	0.14±0.01			
E200R	4.41±0.69	31.5	Loop of the beta sheet	+++
E200A/D201G	3.70±0.17	26.4	Loop of the beta sheet	+++/+++
E233A/N237A	0.24±0.05	1.7	helix5	+/+
S234A/E238A	0.04±0.02	0.3	helix5	+/+
T241A/E245A	0.16±0.03	1.1	helix5	+/++
Q248A	0.11±0.03	0.8	helix5	+
D252A	0.12±0.01	0.9	helix5	++
T249A/T253A	0.17±0.09	1.2	helix5	++/++
K256A	1.30±0.18	9.3	Between helix5 and C-term	+++
R260A	2.1±0.3	15.0	Between helix5 and C-term	+++
R266A	0.21±0.02	1.5	C-term	+++
K268A	0.88±0.09	6.3	C-term	+++
D270A	0.25±0.06	1.8	C-term	++
K273A	0.21±0.04	1.5	C-term	++
ΔC13	0.59±0.06	4.2	C-term truncation	
ΔC28	2499±155	17850	C-term truncation	

CP Beta Subunits	Kd(nM)	Relative affinity (X-fold)	Location of the mutation	Conservation of the amino acid residues
K53A	0.16±0.09	1.1	Between the stalk and the beta sheet	++
D58A	0.11±0.02	0.8	Between the stalk and the beta sheet	++
K142A	0.24±0.04	1.7	Loop of beta sheet	++
K143A	0.20±0.07	1.4	Loop of beta sheet	+
R195A	0.49±0.05	3.5	Beta strand 9	+++
K199A	0.29±0.02	1.1	Beta strand 9	+
D200A	0.20±0.07	1.4	Beta strand 9	+
R215A/D219A	0.32±0.21	2.3	helix5	++/++
N222A/S226A	0.25±0.01	1.8	helix5	+/+
K223A	0.47±0.06	3.4	helix5	++
R225A	1.36±0.13	9.7	helix5	+++
T227A	0.30±0.03	2.1	helix5	++
N229A	0.20±0.04	1.4	helix5	++
E230A/G234A	0.20±0.03	1.4	helix5	++/++
K235A	0.26±0.19	1.9	helix5	+++

CP Beta Subunits	Kd(nM)	Relative affinity (X-fold)	Location of the mutation	Conservation of the amino acid residues
D238A	0.20±0.03	1.4	helix5	++
K237A/N241A	0.10±0.03	0.7	helix5	++
E256A/N260A	0.44±0.23	3.1	tentacle(C-term)	+/+
E256S/N260S	0.36±0.10	2.6	tentacle(C-term)	+/+
L258S/L262S/L266S	9.70±1.02	69.3	tentacle(C-term)	++/++/++
L258S/L262S/A265S/L266S	6.90±1.01	49.3	tentacle(C-term)	++/++/++/++
L258S	1.30±0.36	9.3	tentacle(C-term)	++
L262S	4.00±0.89	28.6	tentacle(C-term)	++
A265S	0.20±0.02	1.4	tentacle(C-term)	++
L266S	2.61±0.36	18.6	tentacle(C-term)	++
ΔC34	33.2±2.26	237.1	C-term truncation	

The K_d values for CP mutants binding to actin were determined by least-square fitting of the model with the Berkeley Madonna program (see Methods). The mutations that caused more than a 3-fold of K_d are highlighted in bold.